

This work was written as part of one of the author's official duties as an Employee of the United States Government and is therefore a work of the United States Government. In accordance with 17 U.S.C. 105, no copyright protection is available for such works under U.S. Law. Access to this work was provided by the University of Maryland, Baltimore County (UMBC) ScholarWorks@UMBC digital repository on the Maryland Shared Open Access (MD-SOAR) platform.

Please provide feedback

Please support the ScholarWorks@UMBC repository by emailing scholarworks-group@umbc.edu and telling us what having access to this work means to you and why it's important to you. Thank you.

Tunable, narrow-band, all-metallic microwave absorber

Cite as: Appl. Phys. Lett. **101**, 141115 (2012); <https://doi.org/10.1063/1.4757282>

Submitted: 20 August 2012 . Accepted: 20 September 2012 . Published Online: 04 October 2012

N. Mattiucci, R. Trimm, G. D'Aguanno, N. Aközbek, and M. J. Bloemer



[View Online](#)



[Export Citation](#)

ARTICLES YOU MAY BE INTERESTED IN

[Ultra-broadband microwave metamaterial absorber](#)

Applied Physics Letters **100**, 103506 (2012); <https://doi.org/10.1063/1.3692178>

[Microwave diode switchable metamaterial reflector/absorber](#)

Applied Physics Letters **103**, 031902 (2013); <https://doi.org/10.1063/1.4813750>

[Switchable metamaterial reflector/absorber for different polarized electromagnetic waves](#)

Applied Physics Letters **97**, 051906 (2010); <https://doi.org/10.1063/1.3477960>

Lock-in Amplifiers
up to 600 MHz



Tunable, narrow-band, all-metallic microwave absorber

N. Mattiucci,^{1,a)} R. Trimm,² G. D'Aguanno,¹ N. Aközbek,¹ and M. J. Bloemer³

¹Aegis Tech., Nanogenesis Division 410 Jan Davis Dr, Huntsville, Alabama 35806, USA

²Miltec Corporation, 678 Discovery Drive, Huntsville, Alabama 35806, USA

³Department of the Army, Charles M. Bowden Laboratory, Redstone Arsenal, Alabama 35898, USA

(Received 20 August 2012; accepted 20 September 2012; published online 4 October 2012)

We exploit the metamaterial properties of a thick metallic grating with extreme sub-wavelength slits on a metallic slab to achieve complete absorption of transverse magnetic polarized microwaves. We measure narrow bands of total absorption (up to 99.9999%) from normal to grazing incidence that can be tuned by varying an air gap between the grating and the slab. Unlike typical absorbers, the structure is mostly metallic with a 97% filling factor, and no absorptive material beside the metal itself is employed. We access the absorption properties of metals in the microwave where they are commonly believed to be perfect reflectors. © 2012 American Institute of Physics. [<http://dx.doi.org/10.1063/1.4757282>]

Commercially available microwave absorbers are based on polymeric materials filled with magnetic particles or open celled foam impregnated with a carbon coating. For most applications, metals in the microwave regime are generally treated as perfect conductors (conductivity $\sigma \rightarrow \infty$) and all field components are set to zero inside the metal¹ implying that an electromagnetic wave impinging a sheet of metal is reflected with basically no absorption losses. This assumption is not always valid, particularly in the extreme sub-wavelength regime where the finite conductivity is important. For example, in Ref. 2, the authors theoretically discuss and experimentally demonstrate that the microwave transmission of a single, extremely narrow ($\sim 100 \mu\text{m}$ and below), slit carved in a metal slab is affected by the finite conductivity of the metal itself, challenging the usual assumption that metals can be treated as perfect conductors in this regime. Microwave absorbers made by structuring metal surfaces in a periodic manner with 1-D or 2-D design have been studied in the past.^{3–7} Our work differs from previous studies on the subject because (a) we do not use any absorbing dielectric in our structure to boost the overall absorption; (b) the metal filling factor of our grating is 97%, i.e., basically close to a homogeneous slab of metal; (c) the measured reflectance minima go down to 0.0001% implying absorption level up to 99.9999%; and (d) the reflectance minima can be tuned by varying the air gap (see Fig. 1 for a schematic representation of the structure investigated).

In two recent publications,^{8,9} it has been demonstrated that a metallic grating of thickness l , slits of width w , and period d , as shown in Fig. 1, can be *rigorously* homogenized as a metamaterial slab of same thickness l and effective constitutive parameters given by the following equations:

$$\varepsilon_{\text{eff}} = \varepsilon_w d/w, \quad \mu_{\text{eff}} = w(\beta_s^2/k_0^2 + \sin^2 \vartheta)/d\varepsilon_w, \quad (1)$$

where ε_{eff} and μ_{eff} are the effective electric permittivity and magnetic permeability of the metamaterial slab, ϑ is the incident angle, ε_w is the dielectric constant of the material

filling the slits ($\varepsilon_w = 1$ in our case), k_0 is the vacuum wave-vector, and β_s is the wave-vector of the fundamental transverse magnetic (TM) guided mode of the parallel plate metal/dielectric/metal waveguides which the grating is made of.

Equation (1) is valid under the assumption of TM-polarized incident radiation (H-field parallel to the grooves of the grating) and that the grating periodicity is smaller than the radiation wavelength ($\lambda > 2d$) so that all diffraction orders, except the zeroth, are evanescent. In the model, we fully take into account the finite conductivity of the metal and the dispersion of β_s (which is a complex number). Following this metamaterial approach, we can assimilate our metallic grating to an effective *magnetodielectric* material, with no electric dissipation, but with *magnetic dissipation* governed by the imaginary part of the effective magnetic permeability: $\text{Im}(\mu_{\text{eff}}) = 2w\text{Re}(\beta_s)\text{Im}(\beta_s)/dk_0^2$. For slit widths of $w > 500 \mu\text{m}$, this term can be neglected in the microwave regime, for the grating thicknesses considered here, due to weak penetration of the fields into the metal¹ and $\text{Re}(\beta_s) \rightarrow k_0$ and $\text{Im}(\beta_s) \rightarrow 0$. For extremely narrow slits, as in the case of the present work, the reduction of the slit width forces more energy into the metal leading to increased losses. In this latter case, the pure transverse electric and magnetic (TEM) mode is transformed into a “plasmonic” TM mode with increased dissipation and slow wave properties,¹⁰ i.e., $\text{Re}(\beta_s) < k_0$ and $\text{Im}(\beta_s) \neq 0$. This dissipation mechanism is quite unusual for the microwave regime and can be used to achieve extremely efficient absorption for polarized waves, as we will show in the following.

Conventional magnetodielectric materials are known to be good microwave absorbers.¹¹ In our case, for the grating described in Fig. 1 with $w = 100 \mu\text{m}$ and $d = 3.275 \text{ mm}$, the effective permittivity and permeability around 13 GHz calculated from Eq. (1) at normal incidence are: $\varepsilon_{\text{eff}} \sim 33$ and $\mu_{\text{eff}} = 0.03 + i1.8 \times 10^{-4}$. For comparison, a conventional microwave absorber material such as FGM-40 in the same frequency range has: $\varepsilon \sim 28 + 2i$, $\mu \sim 1.2 + 1.6i$.¹² The absorption mechanism that we are exploiting here is quite different from that used in conventional microwave

^{a)} Author to whom correspondence should be addressed. Electronic addresses: nadia.mattiucci@us.army.mil and nmattiucci@nanogenesisgroup.com.

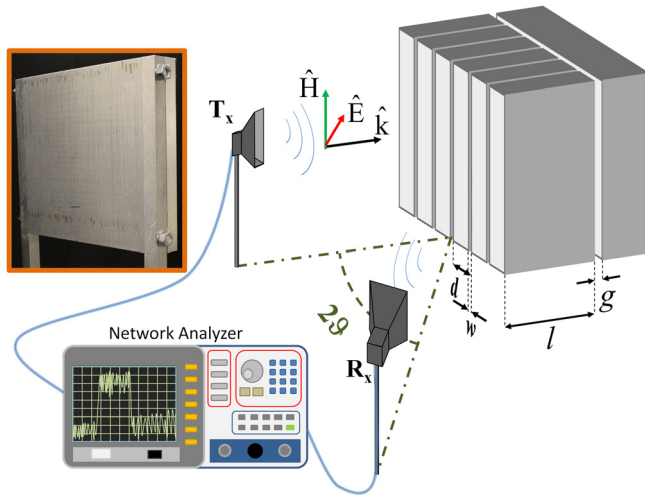


FIG. 1. Schematic representation of the experimental set-up. Inset: picture of the actual sample.

absorber materials. In our case, for particular thicknesses of the grating corresponding to the Fabry-Perot resonances of the effective slab, the field is resonantly funneled inside each slit and strongly “squeezed” with exceptionally high local intensity along the lateral walls of the slits. This phenomenon causes a giant increase in the ohmic losses which ultimately leads to nearly perfect absorption.

Fig. 1 shows the experimental set-up. The grating is made of aluminum bars with $l = 25.4$ mm, $w = 100$ μm , and $d = 3.275$ mm. The overall grating area is 30 cm by 30 cm and is mounted over an aluminum plate having a separation that can be varied with shim spacers placed near the corners of the plate. The individual bars are separated by 100 μm shim spacers positioned near the top and bottom of the grating. Inside the slits, the aluminum surface of each bar had an average roughness of 5 μm as measured by a surface profilometer. The flatness across the surface of the grating was on the order of 100 μm limiting the overall separation between the back plate and the grating to a minimum of ~ 100 μm without any shim in place. Therefore, we define the gap distance as $g = \text{spacer} + 100$ μm . It is worthwhile to underline that the metal filling factor of our grating is $\sim 97\%$, i.e., very close to a homogeneous slab of metal.

Two identical rf horn antennas are used as emitter (T_x) and receiver (R_x) connected to an Agilent (E8363C) vector network analyzer. Reflection measurements were taken from the 18–40 GHz. In Fig. 2, we show the reflected power (reflectance R) in dB for an incident angle of $\vartheta = 50^\circ$. In this case, $g = 431$ μm . We note four narrow-band reflectance dips with a measured minimum ranging from -60 dB (corresponding to absorption $A = 1 - R = 99.9999\%$) to -20 dB (corresponding to 99% absorption).

In Fig. 3, experimental results are compared with theoretical results and numerical simulations for each of the four reflectance resonances found in the range 15–40 GHz. In this case, the reflectance is shown in linear scale from 0 to 1.

The theoretical results are obtained by the transfer matrix technique.¹³ The actual grating of thickness l is replaced with a homogeneous layer of same thickness and effective parameters given by Eq. (1) and the transfer matrix is applied. The

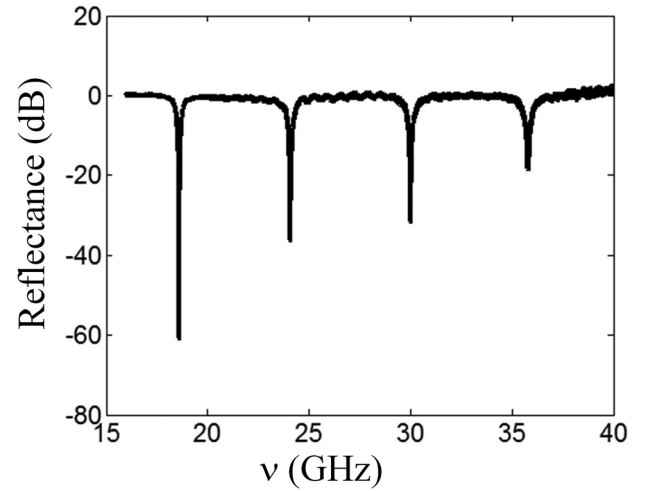


FIG. 2. Measured reflectance in dB ($10\log_{10}R$) vs. frequency for an incident angle $\vartheta = 50^\circ$. The parameters of the structure are: $l = 25.4$ mm, $w = 100$ μm , $d = 3.275$ mm, and $g = 431$ μm .

full-wave numerical calculations are performed with the rigorous Fourier modal method (FMM).¹⁴ The aluminum dispersion in the microwave has been calculated using a lossy Drude model whose parameters (plasma frequency and damping) are chosen according to the experimental data.¹⁵ The figures show an overall good agreement between the positions of the reflectance minima predicted by our theory, those numerically calculated, and the results of the experiment.

We have also measured the angular dependence of the reflectance minima. In Fig. 4(a), we show the dispersion of the reflectance minima calculated according to theory in the (ν, ϑ) plane compared with the experimental results. The solid circles represent the position of the measured reflectance minima. The measured values closely follow the dispersion predicted by the model, and, moreover, the phenomenon spans from near normal to grazing incidence providing great flexibility in terms of angular acceptance. Fig. 4(b) shows the measurements for the first resonance around 18 GHz. It is noted that the resonances blue-shift for increasing incident angles, as one may expect from conventional Fabry-Perot type resonances.

In order to show the possibility to tune the absorption peak, we study next the dependence of the reflectance resonances on the thickness of the air gap g . In Fig. 5(a), we show the dispersion of the reflectance minima in the (ν, g) plane for a fixed incident angle $\vartheta = 20^\circ$. Also, in this case the experimental data closely follow what the theory predicts. The position of the reflectance minima red-shift for increasing values of the air gap g , again this is an expected phenomenon for Fabry-Perot resonances. The structure possesses a good level of tunability and by varying the air gap, each resonance can be tuned over a bandwidth that is approximately half of the bandwidth corresponding to two adjacent minima. Finally, in Fig. 5(b) we show the experimental data for different values of the spacer. The figure also shows the reflectance resonance in the case of no back mirror on the grating and in the case of the back mirror attached to the grating with no spacer in between.

In conclusion, we have reported theoretical considerations, numerical simulations, and experimental results on a

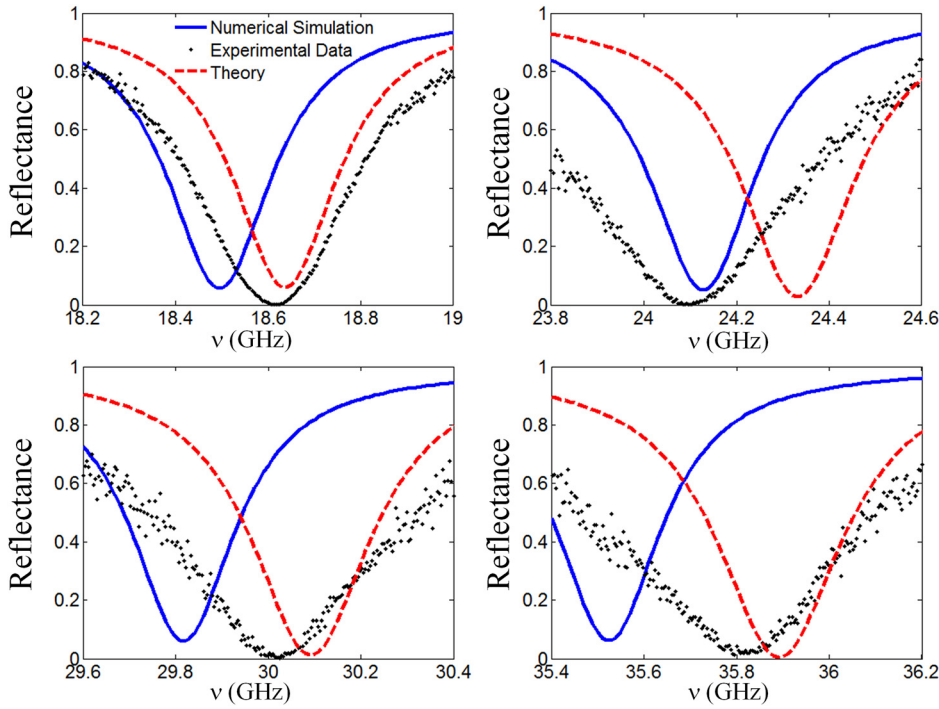


FIG. 3. Comparison between theory, numerical simulation, and experimental data. The grating parameters are reported in Fig. 2.

tunable, all-metallic, wide-angle, perfect microwave absorber based on the metamaterial properties of thick metallic gratings below the first diffraction order. The parameters that have been used in our experiment ($l = 25.4$ mm, $w = 100$ μm , and $d = 3.275$ mm) are not in any way unique.

Many different combinations can yield equivalent results. For example, a sample with a thinner thickness l can be used in conjunction with narrower slit apertures w so that the loss reduction due to a shorter length of the sample is

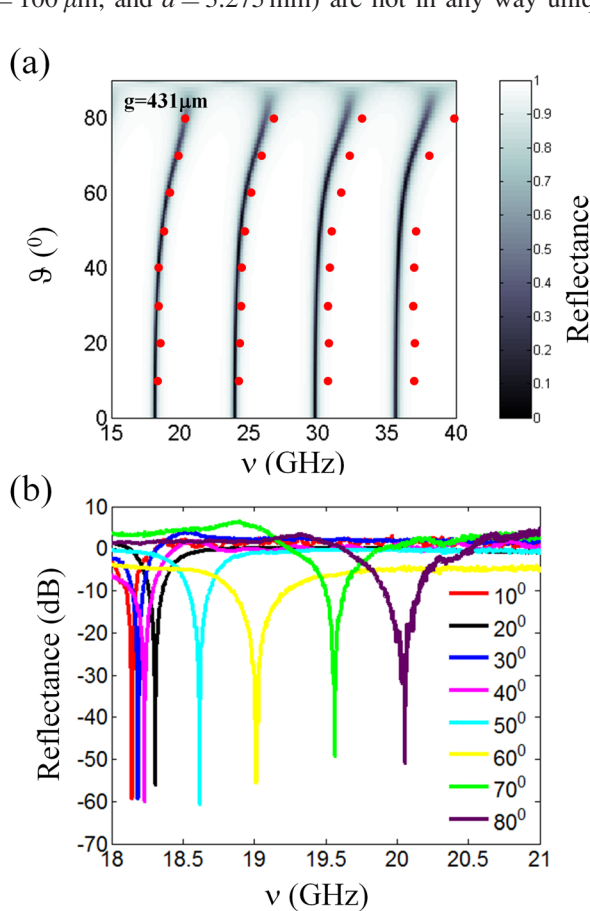


FIG. 4. (a) Reflectance minima (linear scale) in the (ν, θ) plane calculated according to theory compared with the experimental results (solid circles). (b) Experimentally measured reflectance (dB) of the resonance located around 18 GHz for different incident angles.

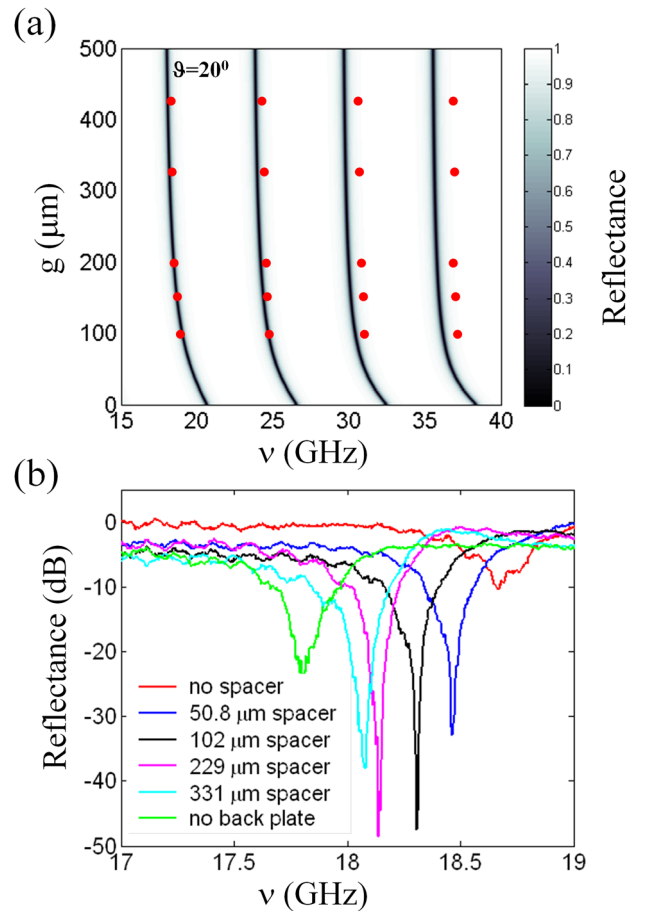


FIG. 5. (a) Reflectance minima (linear scale) in the (ν, g) plane as calculated according to theory compared with the experimental results (solid circles). (b) Experimentally measured reflectance (dB) of the resonance located around 18 GHz for different values of the thickness of the air gap.

compensated by the increased ohmic losses due to the narrower slits. Moreover, although our sample has been made of aluminum, we expect similar results to be valid for other metals as well. We also expect that analogous results could be obtained for a closely spaced array of square metallic tiles (2-D grating), in this case the effect is anticipated to hold for all the incident field configurations in which the polarization of the H-field lays in the plane of the structure. Finally, for possible future applications, we point out that active control of the air gap can be achieved in a fast and effective way by using current piezo technology.

- ¹D. M. Pozar, *Microwave Engineering*, 3rd ed. (John Wiley and Sons Inc., New York, 2005).
- ²J. R. Suckling, A. P. Hibbins, M. J. Lockyear, T. W. Preist, J. R. Sambles, and C. R. Lawrence, *Phys. Rev. Lett.* **92**, 147401 (2004).
- ³A. P. Hibbins, J. R. Sambles, and C. R. Lawrence, *Appl. Phys. Lett.* **80**, 2410 (2002).

- ⁴M. J. Lockyear, A. P. Hibbins, J. R. Sambles, and C. R. Lawrence, *Appl. Phys. Lett.* **83**, 806 (2003).
- ⁵M. J. Lockyear, A. P. Hibbins, J. R. Sambles, and C. R. Lawrence, *Appl. Phys. Lett.* **86**, 184103 (2005).
- ⁶M. J. Lockyear, A. P. Hibbins, J. R. Sambles, P. A. Hobson, and C. R. Lawrence, *Appl. Phys. Lett.* **94**, 041913 (2009).
- ⁷N. I. Landy, S. Sajuyigbe, J. J. Mock, D. R. Smith, and W. J. Padilla, *Phys. Rev. Lett.* **100**, 207402 (2008).
- ⁸A. Alù, G. D'Aguanno, N. Mattiucci, and M. J. Bloemer, *Phys. Rev. Lett.* **106**, 123902 (2011).
- ⁹C. Argyropoulos, G. D'Aguanno, N. Mattiucci, N. Akozbek, M. J. Bloemer, and A. Alù, *Phys. Rev. B* **85**, 024304 (2012).
- ¹⁰G. D'Aguanno, N. Mattiucci, M. J. Bloemer, D. De Ceglia, M. A. Vincenti, and A. Alù, *J. Opt. Soc. Am. B* **28**, 253 (2011).
- ¹¹V. M. Petrov and V. V. Gagulin, *Inorg. Mater.* **37**, 93 (2001).
- ¹²D. K. Ghodgaonkar, V. V. Varadan, and V. K. Varadan, *IEEE Trans. Instrum. Meas.* **39**, 387 (1990).
- ¹³J. Lechner, *Theory of Reflection* (Martin Nijhoff, Dordrecht, 1987).
- ¹⁴L. Li, *J. Opt. Soc. Am. A* **13**, 1870 (1996).
- ¹⁵M. A. Ordal, R. J. Bell, J. R. W. Alexander, L. L. Long, and M. R. Querry, *Appl. Opt.* **24**, 4493 (1985).